JOURNAL OF CATALYSIS 143, 22–31 (1993)

Reversible Activity Enhancement of SiO_2-Supported Group VIII Metal Catalysts by Pretreatment Temperature

JUNJI INUKAI,[1] KIYOTAKA ASAKURA, AND YASUHIRO IWASAWA[2]

Department of Chemistry, Faculty of Science, the University of Tokyo, 7-3-1 Hongo, Bunkyo-ku, Tokyo 113, Japan

Received January 4, 1993; revised April 21, 1993

Reversible enhancement in activity for hydrogenation of ethene, H_2–D_2 equilibrium reaction, and hydrogenolysis of ethane by high-temperature evacuation was observed for Ni, Pd, Pt, Rh, and Ru catalysts. There existed a respective threshold activation temperature (670 ~ 880 K) for each catalyst. Those catalysts were repeatedly used, and this phenomenon was reversible. Change of neither dispersion, particle size, nor particle shape by the high-temperature treatment leading to the enhancement was observed. A strong particle-size dependence of reaction rate for hydrogenation of ethene on Pd/SiO_2 was observed after the catalyst had received the high-temperature treatment, while after low-temperature pretreatment, no dependence of the rate on particle size was observed. Adsorbed CO on the high-temperature treated Rh samples showed much different vibrational spectra from those for the low-temperature treated samples. The threshold enhancement temperature for each metal is related to the sublimation energies. This phenomenon is suggested to arise from roughening of the metal particle surface by the high-temperature treatment. © 1993 Academic Press, Inc.

INTRODUCTION

Modification of metal catalyst surfaces has been studied extensively from scientific interests as well as technological points of view. Some of the examples are addition of promoters (K/Fe (*1*), Li/Pd (*2*)), addition of poisons (S/Fe (*3*)), formation of alloys (Pt–Sn (*4*), Ni–Cu (*5*)), effect of supports (*6*), and so forth. Most of the modification methods and processes reported so far show the irreversible change of the catalytic properties from the unmodified systems induced by the second additives. One example of a reversible catalyst modification is what is called SMSI (strong metal support interaction) (*7*), but the reversible conversion of an SMSI state to a normal state requires the oxidation of samples with O_2 at elevated temperatures, followed by reduction with H_2 at low temperatures. It was reported that the SMSI effect can be effectively used to control and improve reaction selectivities (*8*). It is of interest to study the reversible modification of catalysts merely by heat treatment in order to control the catalytic properties.

The metal atoms on metal surfaces are known to move rather easily from their original locations even at relatively low temperature. One finds examples in the phenomena of roughening transitions (*9*). Roughening transition is referred to as a phase transition. If one can obtain "rough" surfaces with specific coordinatively unsaturated sites unlike those close-packed surfaces, it will provide a good possibility of acquiring catalytically more effective surfaces. Moreover, since the phenomena are indeed physical, the control of catalytic properties is well expected to be reversible. In our experiments, the catalysts were treated at different temperatures and cooled down to room temperature rapidly (less than 1 s) with the wish to retain the surface structure created at high temper-

---

[1] Present address: Department of Chemistry, Faculty of Science and Technology, Keio University, 3-14-1 Hiyoshi, Kohoku-ku, Yokohama 223, Japan.

[2] To whom correspondence should be addressed.

0021-9517/93 $5.00
Copyright © 1993 by Academic Press, Inc.
All rights of reproduction in any form reserved.

ature. We found reversible catalytic enhancement by treating the catalysts at characteristic temperatures which depend on the metal. In this article, the novel behavior of the catalysis of supported metal particles is reported and its origin is discussed.

EXPERIMENTAL

Sample Preparation

Ni/SiO_2, Pd/SiO_2, Pt/SiO_2, Rh/SiO_2, and Ru/SiO_2 were prepared by immersion of SiO_2 (Fuji-Davison Silica Gel No. #952, 300 m^2/g) with aqueous solutions of $NiCl_2$, $PdCl_2$, H_2PtCl_6, $Rh(NO_3)_3$, and $RuCl_3$, respectively, after impregnation for 5 h at room temperature followed by drying at 390 K for 3 h with continuous stirring. The resultant samples were calcined in air at 773 K for 2 h. The metal loading of all the samples was controlled to be 2.0 wt%. Pd/SiO_2 catalysts with different dispersions were also prepared by changing the oxidation temperature and oxidation duration. Each catalyst was oxidized with oxygen (13 kPa) at 673 K for 1 h and subsequently reduced with hydrogen (20 kPa) at 773 K for 1 h *in situ* before each run. The sample was reduced again with 13 kPa of hydrogen at 473 K for 7 min, and evacuated for 0.5 h at given temperatures (base pressure: 2.66×10^{-4} Pa). Then it was rapidly cooled down to 273 K within 1 s using an ice-bath, or otherwise cooled down slowly to room temperature over 0.5 h.

Catalytic Reactions

The catalytic reactions were carried out in a closed circulation system (180 cm^3). Hydrogenation of ethene was conducted under the conditions of $C_2H_4 : H_2 = 3.6 : 7.2$ kPa at 178 k ~ 213 K, and H_2–D_2 exchange reaction was performed with $H_2 : D_2 = 6.7 : 6.7$ kPa at 178 K. Hydrogenolysis of ethane on Rh catalyst was carried out with $C_2H_6 : H_2 = 6.7 : 13.3$ kPa at 449 ~ 488 K. When each run was completed, the catalyst was reduced again with 13 kPa of hydrogen at 473 K for 7 min, evacuated for 0.5 h at a given temperature, and cooled down either rapidly or slowly to be ready for the next run.

Products were analyzed with a gas chromatograph (1.5-m-long columns filled with activated alumina treated with manganese chloride for H_2–D_2 exchange reaction (*10*), or VZ-10 for other reactions).

Characterization

The dispersion of the samples was measured by H_2–O_2 titration (*11,12*). The error in the measurement was ca. 10%. We estimated the particle size, assuming a spherical shape (*13*). TEM (JEOL, JEM1250) was used to observe the change of the shape and size of metal particles. XRD measurements were also carried out to see the morphological change. In order to investigate the local structures of the metal particles, we carried out EXAFS (extended X-ray absorption fine structure) measurements at room temperature and high temperatures using an *in situ* EXAFS cell (*14*) at BL10 of the Photon Factory, KEK (Proposal No. 88022). The experimental conditions and the analytical methods of EXAFS will be described in detail elsewhere (*15*).

IR Measurements

IR spectra of CO adsorbed on Rh catalysts were measured by a double-beam FT-IR spectrometer (JEOL JIR-10). CO was adsorbed at the pressure of 5.3 kPa on the treated catalysts.

RESULTS

Hydrogenation of Ethene on Supported Ni, Pd, Pt, Rh, and Ru Catalysts

With the strategy to modify the catalyst surface for higher activity, as mentioned in the Introduction, the catalysts were evacuated at high temperature and rapidly cooled down. Figure 1 shows the results for Pd. The catalytic activity of Pd/SiO_2 increased by an order of magnitude when evacuated at 773 K and cooled down rapidly to 273 K (within 1 s) (HTT, high temperature treatment) compared to that evacuated at 473 K (LTT, low temperature treatment). The

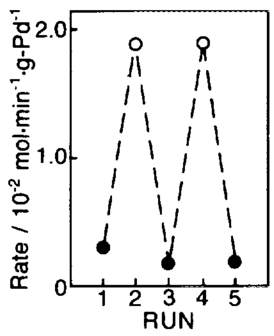

FIG. 1. Reversible activity (initial reaction rate) enhancement/depression of the hydrogenation of ethene at 195 K on Pd/SiO_2 catalyst; C_2H_4 : H_2 = 3.6 : 7.2 kPa. Filled circles (Runs 1, 3, and 5) indicate the results after LTT (473 K evacuation), while open circles (Runs 2 and 4) indicate the results after HTT (773 K).

TABLE 1

The Threshold Temperatures (T_c) for High Activity and the Sublimation Energies (ΔH_f) of Group VIII Metals

	Ni	Pd	Pt	Rh	Ru
T_c (K)	670	670	730	820	880
ΔH_f (kJ/mol)	400	400	560	580	650

catalytic activity was found to depend on the preevacuation temperature, showing the reversible change in Fig. 1. To investigate the suitable temperature for activation, we next changed the evacuation temperature and carried out the reaction. Figure 2 shows the initial rate of ethene hydrogenation on Pd/SiO_2 catalyst against the pretreatment temperature. It was found that a threshold temperature exists for the higher activity around 670 K, where the activity change becomes steep. Below or above this threshold, the activity remained constant. It is notable that this phenomenon was completely reversible as shown in Fig. 1. When the sample was rapidly cooled down and left under vacuum at RT for 14 h, the activity remained almost as high as that evacuated at 773 K (run 9 in Fig. 2). On the other hand, when the sample was evacuated at 773 K and cooled down slowly (about 30 min), the activity decreased to the level for the catalysts treated at 473 K (run 10 in Fig. 2). When the sample was evacuated at 773 K, cooled down rapidly (HTT) to 273 K, and again heated at 473 K for 0.5 h, the catalyst lost its high activity. After the catalyst was evacuated at 473 K, whether cooling down rapidly or slowly gave no influence on the activity, and it remained at the lower level. Thus evacuating the Pd catalyst at a temperature higher than the threshold and cooling it down rapidly before the reaction created the highly active state of the catalyst.

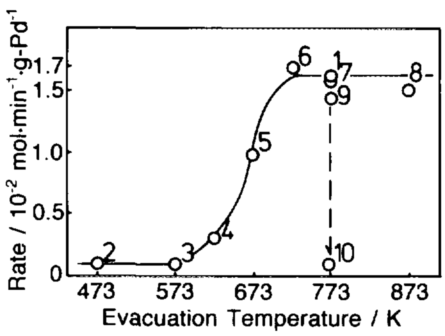

FIG. 2. Initial rate of the hydrogenation of ethene at 195 K on Pd/SiO_2 catalyst after various pretreatment conditions; C_2H_4 : H_2 = 3.6 : 7.2 kPa. Runs 1–8 were carried out in the order after evacuation at various temperatures followed by rapid cooling down to 273 K (within 1 s) except for run 10. Run 9 was carried out after evacuation at 773 K, rapidly cooled down, and left under vacuum at room temperature for 14 h. Run 10 was carried out after evacuation at 773 K and cooled down slowly (ca. 30 min).

The same experiments were also conducted with Ni/SiO_2, Pt/SiO_2, Rh/SiO_2, and Ru/SiO_2. Similar reversible activity-enhancement phenomena were observed in all cases, and the rate of reaction increased by 5 ~ 30 times after HTT. The threshold temperatures were 670, 670, 730, 820, and 880 K for the Ni, Pd, Pt, Rh, and Ru catalysts, respectively. The order of the threshold temperatures corresponds to the order of sublimation energies of these metals (Table 1).

Some differences were found on Rh and

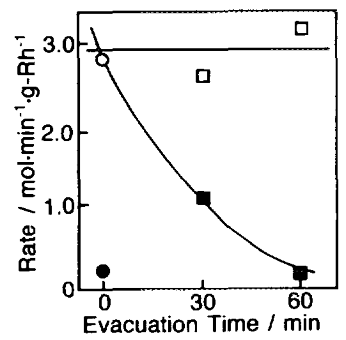

FIG. 3. Initial rate of the hydrogenation of ethene at 195 K on Rh/SiO$_2$ catalyst; $C_2H_4 : H_2 = 3.6 : 7.2$ kPa. (1) Filled circle, evacuated at 673 K; (2) open circle, evacuated at 873 K (HTT); (3) filled squares, evacuated at 673 K after HTT; (4) open squares, evacuated at 473 K after HTT.

Ru catalysts. Rapid cooling within 1 s using an ice-bath was needed for Ni, Pd, and Pt catalysts to reach the higher activated state, without which the activity remained low. However, for Rh and Ru, rapid cooling to 273 K was not necessary for getting the high activity. Simple evacuation above 820 K for Rh and 880 K for Ru was sufficient to activate these two catalysts. To investigate the influence of the temperature on the activated Rh catalyst, the following experiments were carried out. First the catalyst was activated by high temperature evacuation (873 K), and subsequently evacuated at 473 K for 0.5 h or 1 h before the catalytic reaction. The catalyst still maintained the high activity even after the 473 K-evacuation process, as shown in Fig. 3. On the other hand, evacuation for 1 h at 673 K was effective enough to diminish its high-activity state. Thus it is supposed that for Rh and Ru catalysts, the annealing temperature effective for releasing the activated state to the low-activity state is higher than that for Ni, Pd, and Pt catalysts.

The activation energies for ethene hydrogenation on the Pt and Rh catalysts before and after the activation treatment (HTT) (low- and high-activity state) were obtained. No change in the activation energies was observed between both samples with two different activity levels. The activation energy for Pt was 39 kJ/mol and that for Rh was 35 kJ/mol, which corresponded to the values in the literature (*16–18*).

H_2–D_2 Exchange Reaction on Pt/SiO$_2$

H_2–D_2 exchange reaction was performed on Pt/SiO$_2$. A change of activity by HTT was also observed. A similar dependence of the reaction rate on the pretreatment temperature as that observed in the case of hydrogenation of ethene was found.

Hydrogenolysis of Ethane on Rh/SiO$_2$

The hydrogenolysis of ethane on the Rh/SiO$_2$ catalyst was investigated in the temperature range 449 ~ 488 K since the activated state of Rh was found to be stable at 473 K (Fig. 3). The results are shown in Fig. 4. The catalyst treated by HTT (873 K) showed the higher reaction rate than that treated by LTT (673 K). The activation energy for the LTT sample was calculated to be 142 kJ/mol, which well coincides with the values reported (*19,20*), and the reaction rate also coincides with the values previously reported (*19*). On the other hand, when treated at 873 K (HTT) before the reaction, the activation energy was markedly lower at 95 kJ/mol, which is the lowest value ever reported.

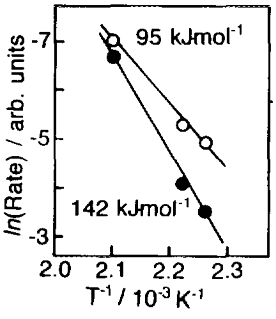

FIG. 4. The hydrogenolysis of ethane on Rh/SiO$_2$ with $C_2H_6 : H_2 = 6.7 : 13.3$ kPa at 449–488 K. Filled circles, LTT (142 kJ/mol); open circles, HTT (95 kJ/mol).

TABLE 2

The Dispersions (H/M) and Particle Sizes of the LTT and HTT Samples by H_2–O_2 Titration and TEM

Ni	LTT (473 K)	HTT (773 K)
Dispersion (%)	12	11
Size (dispersion) (nm)	8.5	9.3
Pd	**LTT (473 K)**	**HTT (773 K)**
Dispersion (%)	5	5
Size (dispersion) (nm)	20	20
Size (TEM) (nm)	15	16
Pt	**LTT (473 K)**	**HTT (773 K)**
Dispersion (%)	17	18
Size (dispersion) (nm)	6.7	6.3
Size (TEM) (nm)	6	6
Rh	**LTT (673 K)**	**HTT (873 K)**
Dispersion (%)	38	34
Size (dispersion) (nm)	2.7	3.1
Size (TEM) (nm)	3	3
Ru	**LTT (723 K)**	**HTT (923 K)**
Dispersion (%)	8	8
Size (dispersion) (nm)	13	13

TABLE 3

Turnover Frequencies for Hydrogenation of Ethene at 195 K on the HTT and LTT Samples

	Ni	Pd	Pt	Rh	Ru
LTT (min^{-1})	2.2	1.8	0.5	8.6	3.0
HTT (min^{-1})	12	35	12	103	83

Note. $C_2H_4 : H_2 = 3.6 : 7.2$ kPa.

Characterization of the Samples

Table 2 shows the dispersions and particle sizes of the samples after LTT and HTT by H_2–O_2 titration and TEM. For all the catalysts, within the accuracy of our experiments, no change of dispersion was observed between the LTT and HTT samples. TEM observation revealed that the particle shapes were mostly spherical, and semispherical shapes appeared in part. The average particle sizes (*13*) from our dispersion measurements coincided with the results of TEM. Using the dispersions of catalysts, the turnover frequencies (TOF) for ethene hydrogenation were calculated in Table 3. The rate of reaction after HTT was found to be generally greater than the reported values (*16, 17*).

Little change of the intensity, peak patterns, or peak width in the X-ray diffraction was observed between LTT and HTT.

Extended X-ray absorption fine structure (EXAFS) measurements were carried out at room temperature *in vacuo* in order to investigate the difference of atom–atom distances and coordination numbers between the HTT and LTT samples. The EXAFS analysis for Pd, Pt, Rh, and Ru particles on SiO_2 is shown in Table 4. However, there is no significant difference between HTT and LTT in coordination numbers or in interatomic distances.

EXAFS Measurements under in situ Conditions

EXAFS measurements of Rh/SiO_2 were carried out not only at room temperature, but also at various temperatures up to 823 K under *in situ* conditions. No significant change in coordination numbers or in interatomic distances was observed. However, the Debye–Waller factor increased with temperature. The Debye–Waller factors for Rh/SiO_2 for a typical sample, as derived from the ratio method (*21*), are shown in Fig. 5 as a function of measurement temperatures together with the results of a Rh foil. The Debye–Waller factor was estimated to involve the error bar of 2×10^{-4} nm in the present systematic analyses. In the case of Rh particles on SiO_2, the Debye–Waller factor gave an inflection point at 770 K, corresponding to the temperature where the enhancement in activity starts. The Debye–Waller factor for a Rh foil increased continuously with temperature as usual, because of the increase in thermal disorder. The increasing rate of the Debye–Waller factor with temperature depends on the fre-

TABLE 4

The Results of EXAFS Analysis for HTT and LTT Catalysts

Pd	LTT (473 K)	HTT (773 K)	(Bulk XRD)
Atom–atom distance (nm)	0.275	0.274	(0.2745)
Coordination number	11.8	11.7	(12)
Pt	LTT (473 K)	HTT (773 K)	(Bulk XRD)
Atom–atom distance (nm)	0.277	0.277	(0.2770)
Coordination number	11.1	10.9	(12)
Rh	LTT (673 K)	HTT (873 K)	(Bulk XRD)
Atom–atom distance (nm)	0.268	0.268	(0.2685)
Coordination number	8.7	8.8	(12)
Ru	LTT (473 K)	HTT (773 K)	(Bulk XRD)
Atom–atom distance (nm)	0.267	0.268	(0.2678)
Coordination number	11.2	11.2	(12)

Note. Coordination number: ±0.5.

quency and hence force constant of the metal–metal bond (*21*). The abrupt increase in frequency indicates the weakening of metal–metal bonding. Although we should consider these data carefully, we can safely say that some change in the dynamic property of the particle surfaces occurs at this temperature. Further accurate analyses are now proceeding (*15*).

Particle Size Effect in Hydrogenation of Ethene on Pd/SiO$_2$

The particle size effect in hydrogenation of ethene (*18, 22*) was examined on Pd/SiO$_2$ catalysts with or without the activation treatment. The average particle sizes were estimated by H$_2$–O$_2$ titration (*12, 13*). The results are presented in Fig. 6. The TOFs for the LTT catalysts did not change with increasing particle sizes. The rate was the same as the ones reported before. On the other hand, when they had gone through HTT, the sample with the average size of ca. 20 nm showed the highest activity. The ones with the smallest (3 nm) and largest (41 nm) particle sizes showed no activity

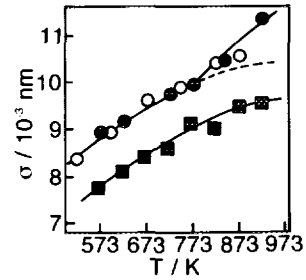

FIG. 5. Debye–Waller factor at temperatures 527–923 K. Filled square, Rh foil; filled circle, Rh/SiO$_2$ as temperature was increased; open circle, Rh/SiO$_2$ as temperature was decreased.

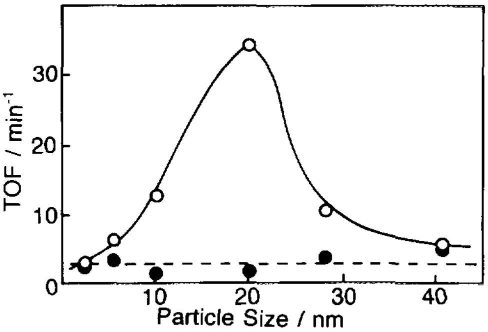

FIG. 6. Size dependency on the catalytic activity of HTT (open circle) and LTT (filled circle) on Pd/SiO$_2$ catalysts with C$_2$H$_4$: H$_2$ = 3.6 : 7.2 kPa at 195 K.

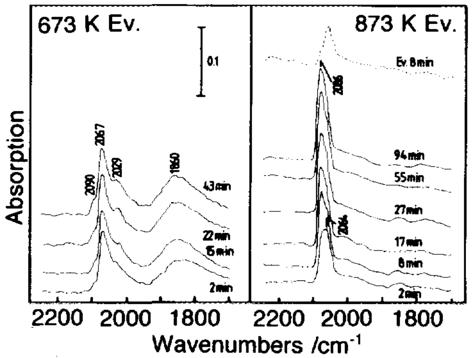

FIG. 7. IR spectra of adsorbed CO on Rh/SiO_2 catalyst after LTT (left) and HTT (right), respectively. The dotted spectrum in the right part is the spectrum after evacuation for 8 min at room temperature.

change with or without HTT. We examined the threshold temperature for activation of the catalysts with the particle sizes 10 ~ 28 nm, and found no change of it (670 K) according to the particle size was observed.

IR Measurements

Figure 7 shows IR spectra of adsorbed CO on the Rh catalyst after the high (873 K) and low (673 K) temperature evacuation. Time dependency of the intensity is also shown in the figure. When Rh was exposed to CO after LTT, an IR spectrum of CO on Rh with the peaks at 2090, 2067, 2029, and 1860 cm^{-1} was observed. The peak at 2067 cm^{-1} is assigned to on-top CO, the peaks at 2029 and 2090 cm^{-1} to twin CO, and the peak at 1860 cm^{-1} to bridged CO (*23*). The intensity of the twin CO and bridged CO gradually increased. On the other hand, the sample after HTT showed completely different spectra. The CO at 2064 cm^{-1} first adsorbed, and another peak at 2086 cm^{-1} kept growing and was saturated in an hour. This peak could be easily removed by evacuation at room temperature, as shown in Fig. 7. No peak ascribed to bridged CO was observed.

DISCUSSION

The reversible enhancement/depression phenomena could be explained by the following reasons:

(i) Reversible change of surface areas and particle sizes after HTT and LTT.

(ii) Effect of contamination. High temperature evacuation might remove the contamination on the surface to lead to the higher activity.

(iii) Surface morphological change by the heat treatment.

We discuss these three possibilities.

(i) In regard to an increase of surface areas by HTT, we did not observe changes in dispersion within an error of 10%. Again, TEM, XRD, and EXAFS data demonstrate that the particle sizes were not changed, with neither sintering nor redispersion taking place. Thus, enhancement of the reaction rates cannot be explained simply by an increase of the surface area.

(ii) The effect of contamination may not well explain the phenomena, either. After the catalysts were evacuated at high temperature and cooled down rapidly (HTT), the TOFs became greater than the reported values (Table 3). Moreover, the activity remained at almost the same high level even after hours (Fig. 2). If the residual gases readsorbed on the surface and deactivated it, the samples should lose their activities in a certain period at RT, whether cooled down rapidly or slowly. However, this was not the case. The catalysts treated at high temperature and cooled down rapidly showed high activity even after keeping them for hours at room temperature, while the catalysts treated at high temperature and cooled down slowly (in 30 min) lost their high activity. This indicates that the enhancement of the activity does not arise from the removal of poison on the surface by HTT.

(iii) Here, we propose a new possibility, i.e., the surface morphological change by HTT just as we intended. A metal surface reversibly roughens at a lower temperature than its melting point (*9*). For example, the melting point of Ni is 1720 K, while the roughening temperature (transition temperature) of Ni(115) was estimated to be 450 K (*9*). A similar roughening transition should happen on the surface of metal particles on supports. The EXAFS coordination number of Rh–Rh remained unchanged before and after the break in the Debye–Waller factor vs temperature plot, which may exclude the bulk phase transition. Rather, the break suggests a surface morphological change involving a phase transition of the top and second layers at Rh particle surfaces. In the usual case, the surface turns back to its stable state in the cooling process. However, when it is cooled down rapidly just like in our case, the roughened surface state may be maintained. Moreover, fine particles may have some ability to keep their high temperature states when cooled down rapidly. In fact, Fe particles smaller than 40 nm maintain its γ-phase when quenched from 1270 K to room temperature in vacuum (*24, 25*), while bulk Fe has never been found to have γ-phase even cooled down rapidly. Thus the small particles in the present catalysts which are roughened at high temperatures can maintain their rough surfaces during and after the rapid cooling (within 1 s). In this context, we should consider the disappearance of the reversible enhancement phenomenon for Pd/SiO_2 particles with diameters less than 3 nm. It is reported that the Au particles less than 2 nm are observed to be changing their morphologies continuously at room temperature under limited conditions of TEM (*26, 27*). Pd particles less than a specific critical size (3 nm) might easily change their structures during the rapid cooling or even at room temperature, leading to the disappearance of the phenomenon. No observation of the high-temperature treatment effect for the 41-nm Pd particle may be due to the high heat capacity as compared to the smaller particles, which prevents the particles cooling down rapidly enough in the present procedure. The particle size effect in ethene hydrogenation was observed by using larger Pd particles than those usually employed and by the high temperature treatment.

The transition temperature for the enhancement of the catalytic activity is correlated to the sublimation energy corresponding to the binding energy of surface atoms. Therefore, as the sublimation energy becomes smaller, atoms on the surface become mobile at a lower temperature.

The IR data of CO give information on surface morphological change after the high temperature treatment. After the evacuation of Rh/SiO_2 at 873 K, the bridged CO peak at 1860 cm^{-1} was completely lost in Fig. 6. On the other hand, the new peak at 2086 cm^{-1} appeared and grew slowly to reach its saturation after an hour, without a significant shift. The new peak disappeared soon after the evacuation of CO at room temperature, suggesting that the CO molecules corresponding to the new peak are weakly bound to the Rh surface. The disappearance of the bridged CO peak can be explained by the disappearance of flat ensembles on the Rh particles. The oxidative fragmentation of Rh particles on SiO_2 by CO adsorption under the present conditions did not occur according to EXAFS. The *in situ* EXAFS data revealed that there is a discontinuous increase in the Debye–Waller factor in Fig. 6, and that the inflection point in the Debye–Waller factor vs the evacuation temperature plots is the same as the threshold temperature for the higher activity state. It is supposed that the discontinuous increase of the Debye–Waller factor reflects the roughening transition of the particle surfaces. The roughening transition at the surface would produce a new kind of disorder having adatom sites. The resultant surface may be active for CO dissociation at room temperature to form O(ad) atoms. The neighboring Rh atoms possess a positive charge which causes an upward shift of CO IR peaks. Alternatively, the CO-peak shift can be explained in the following manner. The calculation of Thompson and Huntington (*28*) based on the jellium model suggested that the step edge on the surface possesses cationic character. Thus, the adatom sites may possess a positive charge.

Hydrogenolysis of ethane is known as a typical structure-sensitive reaction (*18, 19*) where the reaction rate increases as the particle size decreases. It is explained by the existence of unsaturated sites, or defect sites. Also the studies using single crystals have demonstrated the importance of the step and kink sites (*29*). In the hydrogenolysis of ethane on Rh/SiO_2 after the high temperature treatment (HTT), not only the increase of reaction rate but also the decrease of activation energy was observed. This fact supports the atomic-scale surface modification by the high temperature treatment. Hydrogenation of ethene is not usually considered to be a structure-sensitive reaction (*18*). However, there are some reports showing structure sensitive characters. Masson *et al.* (*30*) gave an example of a structure sensitivity of the hydrogenation of ethene on Pt particles deposited on single crystals of oxides. They showed that the particles of 0.6 nm in amorphous phase were most active. Farnsworth *et al.* (*31*) bombarded Pt and Ni films with Ar^+, carried out the hydrogenation of ethene, and obtained a high activity which could not be explained by the surface area change. Increase of TOF of ethene hydrogenation was suggested to be due to the surface defects produced by the bombardment of Ar^+. Thus the roughening of the surface structure can enhance the catalytic activity for ethene hydrogenation.

CONCLUSIONS

A new way to modify metallic catalysts supported on SiO_2 was described. Simply, evacuation at high temperature and rapid cooling was necessary for the higher reaction rate of hydrogenation of ethene, hydrogenolysis of ethane, and H_2–D_2 exchange reaction. Macroscopic change of particles such as particle sizes, bond distances, and bond coordination numbers could not be detected. Considering also the results of IR spectra of adsorbed CO, the origin of the reversible enhancement of activity by the high temperature treatment was proposed to be due to surface roughening and its quenching. These phenomena are characteristic of fine metal particles of proper sizes.

ACKNOWLEDGMENT

The authors thank Dr. H. Tsunakawa of the University of Tokyo for TEM measurements.

REFERENCES

1. Arakawa, H., and Bell, A. T., *Ind. Eng. Process. Des. Dev.* **22,** 971 (1983).
2. Rieck, J. S., and Bell, A. T., *J. Catal.* **100,** 305 (1986).
3. Karn, F. S., Shultz, J. F., Kelly, R. E., and Anderson, R. B., *Ind. Eng. Chem. Prod. Res. Dev.* **2,** 43 (1963).
4. Dautzenberg, F. M., Helle, J. N., Biloen, P., and Satchtler, W. M. H., *J. Catal.* **63,** 199 (1980).
5. Ponec, V., and Sachtler, W. M. H., *in* "Proceedings, 5th International Congress on Catalysis, Palm Beach, 1972" (J. W. Hightower, Ed.), p. 645. North-Holland, Amsterdam, 1973.
6. Asakura, K., and Iwasawa, Y., *Chem. Lett.*, 633 (1988).
7. Tauster, S. T., Fung, S. C., and Garten, R. L., *J. Am. Chem. Soc.* **100,** 170 (1978); Tauster, S. T., and Fung, S. C., *J. Catal.* **55,** 29 (1978); Tauster, S. T., Fung, S. C., Baker, R. T. K., and Horsley, J. A., *Science* **211,** 1121 (1981).
8. Yoshitake, H., Asakura, K., and Iwasawa, Y., *J. Chem. Soc. Faraday Trans. 1* **85,** 2021 (1989); Yoshitake, H., and Iwasawa, Y., *J. Catal.* **125,** 227 (1990).
9. Villain, J., Grempel, D. R. and Lapujoulade, J., *J. Phys. F: Met. Phys.* **15,** 809 (1985); Conrad, E. H., Aten, R. M., Kaufman, D. S., Allen, L. R., and Engel, T., *J. Chem. Phys.* **84,** 1015 (1986); Nijs, M., Riedel, E. K., Conrad, E. H., and Engel, T., *Phys. Rev. Lett.* **57,** 1279 (1986); Gong, Y. M., and Gorner, R., *J. Chem. Phys.* **86,** 1359 (1988).
10. Yasumori, I., and Ohno, S., *Bull. Chem. Soc. Jpn.* **39,** 1302 (1966).
11. Doring, T. A., Burlace, C. J., and Moss, R. L., *J. Catal.* **12,** 207 (1968).
12. Benson, J. E., Hwang, H. S., and Boudart, M., *J. Catal.* **30,** 146 (1978).
13. Anderson, J. R., "Structure of Metal Catalysts," p 358, Academic Press, London, 1975.
14. Iwasawa, Y., Asakura, K., Ishii, H., and Kuroda, H., *Z. Phys. Chem. N. F.* **144,** 105 (1985); Asakura, K., and Iwasawa, Y., *J. Phys. Chem.* **93,** 4213 (1989).
15. Asakura, K., Inukai, J., and Iwasawa, Y., submitted for publication.
16. Gallezot, P., *Catal. Rev.-Sci. Eng.* **20,** 121 (1979).
17. Beeck, O., *Discuss. Faraday Soc.* **8,** 118 (1950).
18. Boudart, M., *in* "Proceedings, 6th International Congress on Catalysis, London, 1976" (G. C. Bond, P. B. Wells, and F. C. Tompkins, Eds.), Vol. 1, p. 1. The Chemical Society, London, 1977.
19. Yates, D. J. C. and Sinfelt, J. H., *J. Catal.* **8,** 348 (1967).

20. Sinfelt, J. H., and Yates, D. J. C., *J. Catal.* **8,** 82 (1967).

21. Yokoyama, K., Asakura, Y., Iwasawa, and H. Kuroda, *J. Phys. Chem.* **93,** 8323 (1989).

22. Schlatter, J. C., and Boudart, M., *J. Catal.* **24,** 482 (1972).

23. Zhong, S.-H., *J. Catal.* **100,** 270 (1986).

24. Fukano, Y., *Bul. Jpn. Inst. Met.* **15,** 639 (1976).

25. Kusunoki, M., and Ichikawa, T., *Jpn. J. Appl. Phys.* **25,** L219 (1986).

26. Iijima, S., and Ichihashi, T., *Phys. Rev. Lett.* **56,** 616 (1988).

27. Berry, R. S., *in* "Microclusters" (S. Sugano, Y. Nishida, and S. Ohnishi, Eds.), p. 200. Springer-Verlag, Berlin, 1987.

28. Thompson, M. D., and Huntington, H. B., *Surf. Sci.* **116,** 522 (1982).

29. Egawa, C., and Iwasawa, Y., *Surf. Sci.* **198,** L329 (1988).

30. Masson, A., Bellamy, B., Colomer, G., M'Bedi, M., Rabette, P., and Che, M., *in* "Proceedings, 8th International Congress on Catalysis, Masson, A., Bellamy, B., Romdare, Y. H., Che, M., Roulet, H., and Dufour, G., *Surf. Sci.* **173,** 479 (1986).

31. Farnsworth, H. E., and Woodcock, R. F., *Adv. Catal.* **9,** 123 (1957).